Impact of Low-Temperature Plasmas on *Deinococcus radiodurans* and Biomolecules

Rakesh Mogul,[†] Alexander A. Bol'shakov,[‡,§] Suzanne L. Chan,[†] Ramsey M. Stevens,[⊥] Bishun N. Khare,[||] M. Meyyappan,[#] and Jonathan D. Trent[†,*]

Astrobiology Technology Branch, Plasma Research Group, Center for Nanotechnology, NASA Ames Research Center, Moffett Field, California 94035, Eloret Corporation, Sunnyvale, California 94087, and SETI Institute, Mountain View, California 94043

The effects of cold plasma on *Deinococcus radiodurans*, plasmid DNA, and model proteins were assessed using microbiological, spectrometric, and biochemical techniques. In low power O_2 plasma (~25 W, ~45 mTorr, 90 min), *D. radiodurans*, a radiation-resistant bacterium, showed a 99.999% reduction in bioburden. In higher power O_2 plasma (100 W and 500 mTorr), the reduction rate increased about 10-fold and observation by atomic force microscopy showed significant damage to the cell. Damage to cellular lipids, proteins, and chromosome was indicated by losses of infrared spectroscopic peaks at 2930, 1651, 1538, and 1245 cm^{-1}, respectively. In vitro experiments show that O_2 plasmas induce DNA strand scissions and cross-linking as well as reduction of enzyme activity. The observed degradation and removal of biomolecules was power-dependent. Exposures to 200 W at 500 mTorr removed biomolecules to below detection limits in 60 s. Emission spectroscopy indicated that *D. radiodurans* cells were volatilized into CO_2, CO, N_2, and H_2O, confirming that these plasmas were removing complex biological matter from surfaces. A CO_2 plasma was not as effective as the O_2 plasma, indicating the importance of plasma composition and the dominant role of chemical degradation. Together, these findings have implications for NASA planetary protection schemes and for the contamination of Mars.

Introduction

Surface sterilization is important in a variety of endeavors, including medicine (*1*, *2*), some electronics, and more recently, NASA's astrobiology missions to search for life beyond Earth (*3*, *4*). The killing and removal of microorganisms and biomolecules from surfaces have traditionally been accomplished by techniques that use heat, chemicals, and/or various forms of radiation (*5*−*7*). Better means for detecting microorganisms and biomolecules, however, have revealed that these established techniques are less effective than previously believed (*8*−*11*) and has stimulated research into new techniques (*12*−*15*).

Sterilization methods using low-temperature plasmas have gained recognition for their efficacy and low costs (*16*−*19*). Generated in gases such as O_2, N_2, CF_4, CO_2, and air, they are generally described as nonthermal kinetic equilibrium processes that result in the production of neutral and ionic species, free electrons, and ultraviolet (UV) radiation. It is through the combined effects of plasma processes such as chemical degradation, UV photodesorption, and ion bombardment that cause the destruction of microorganisms and organic matter (*19*, *20*). These plasmas typically induce surface temperatures of <100 °C and are therefore useful in sterilizing and cleaning the surfaces of devices that are sensitive to high temperatures.

For NASA, decontamination of space probes is important both to preserve extraterrestrial environments (*21*, *22*) and to avoid interference with experiments designed to detect life or chemical evolution beyond Earth (*3*, *23*). Of particular concern are microorganisms, viruses, and biomolecules that can survive the low-pressure and high-radiation environments of interplanetary space or the conditions in areas of interest such as Mars or Europa. *Deinococcus radiodurans* can survive desiccation and ionizing radiation of 60 Gy/h for 30 h with no loss of viability (*24*, *25*), making this microbe a plausible candidate for surviving interplanetary travel.

Whereas the biological effects of reactive oxygen species (*26*−*28*) and UV radiation (*29*, *30*) have been studied in detail, the biomolecular effects of low-temperature plasmas have yet to be elucidated. We have studied the effects of O_2 plasma on *D. radiodurans* and on the destruction and removal of specific biomolecules from surfaces. We measured the effects of plasma power (25−250 W) and composition (O_2 and CO_2) on the survival and stability of *D. radiodurans* cells and on the function and stability of either DNA or model proteins (bovine serum albumen and soybean lipoxygenase). The results contribute to the mechanistic understanding of low-temperature

* To whom correspondence should be addressed. Tel: (650) 604-3686. Fax: (650) 604-1092. Email: jtrent@mail.arc.nasa.gov.
[†] Astrobiology Technology Branch.
[‡] Plasma Research Group.
[#] Center for Nanotechnology.
[⊥] Eloret Corporation.
[||] SETI Institute.
[§] National Research Council Associate on leave from the Institute of Physics, St. Petersburg State University, St. Petersburg, 198904 Russia.

10.1021/bp025665e CCC: $25.00
Published on Web 00/00/0000

plasma induced sterilization, degradation, and removal of biological matter from surfaces.

Experimental Procedures

Materials. *Deinococcus radiodurans* strain R1 was obtained from ATCC and stored as glycerol stocks at −80 °C. Growth media were prepared as described in Venkateswaran et al. (*25*). Plasmid DNA (pRc/CMV2) and bovine serum albumen (BSA) were purchased from Sigma. Soybean lipoxygenase-1 (SLO) and linoleic acid were obtained from the Holman Research Group (U.C. Santa Cruz). Oxygen gas was purchased from AirGas (99.9%) and Scott Specialty Gases (99.99%). A Martian atmospheric gas analogue (MAG) containing 95.48% CO_2, 2.51% N_2, and 2.01% Ar was obtained from Matheson Gas. Hanging drop slides were obtained from Fisher Scientific. Potassium bromide optical windows (25 mm × 4 mm) were purchased from Harrick Scientific Corporation. All materials were of highest grade, and pure water (18 MΩ cm^{-1}) was used throughout.

Plasma Reactors. Two different plasma reactors were used in this study: a low power (∼25 W) barrel reactor (PLASMOD, Tegal Corporation) was used for a majority of the microbiological experiments, and a custom-built reactor (ARC-PR) with optimal running conditions of ≥50 W was used for experiments involving molecular and structural characterizations. In all cases, the plasmas were capacitively coupled, low temperature ($T_e = 5-12$ eV), and powered by a 13.56 MHz radio frequency (Bol'shakov et al., unpublished results).

The ARC-PR was constructed by the plasma research group at the NASA Ames Center for Nanotechnology and was designed to allow high-throughput exposures of biological samples through the use of two connecting chambers—a load-lock and reaction chamber—separated by a moveable gate. Typically, the biological sample was placed into the load-lock chamber, the pressure was reduced to ∼20 mTorr, and the target gas was introduced to final pressure of 500 mTorr. The gate was then opened, and the sample was moved into the reaction chamber, which contained the stabilized plasma discharge. After exposure, the sample was shifted back to the load-lock chamber, the gate was closed, and the pressure was readjusted to 1 atm using dry air. Samples were then analyzed using microbiological, spectrometric, and/or biochemical techniques. A thermocouple on the lower electrode measured surface temperatures during plasma exposures. In all cases, the plasmas were tuned to yield a reflected power of <3% of the forward incident power. Power is reported as the difference between the incident and reflected powers.

Microbe Exposure. *Deinococcus radiodurans* was grown in TGY medium to mid-log phase (∼10^8 cells/mL) at 30 °C. Cells were diluted to 5 × 10^7 cells/mL in minimal medium, and 100 μL was transferred onto a 25 mm (0.4 μm) Nuclepore membrane and dried on a 7.0 cm Whatman filter. The inoculated membrane was transferred to a glass Petri dish and inserted into the PLASMOD reactor. The pressure within the reactor was reduced to ∼20 mTorr, and O_2 was introduced at a flow rate of 1.02 cm^3/min to a final pressure of ∼45 mTorr. The chamber was equilibrated for ∼30 min, the radio frequency power was applied (∼25 W), and the inoculated membrane was exposed to the plasma for differing durations (10−90 min). Throughout all exposures, the temperature within the plasma chamber never rose to above ∼50 °C.

After each exposure, the membrane was placed into 0.5 mL of minimal medium and gently vortexed to remove the cells, and serial dilutions were plated onto TGY/agar plates. Plates were incubated for 3 days at 30°C, colonies were counted, and survival was assayed using the most probable numbers method. An additional survival experiment was performed using the ARC-PR at 100 W and 500 mTorr for 60 s. Control experiments assaying the effects of drying, reduced pressure, and O_2 flow on the survival of the cells as well as the percent recovery from the membranes were also run. All experiments were done in triplicate except for the 60- and 90-min runs using the PLASMOD, which were done in duplicate.

Atomic Force Microscopy. A mid-log phase culture of *D. radiodurans* was washed twice in water by centrifugation (10,000 rpm, 30 s). A suspension of ∼7 × 10^9 cells/mL was prepared in water, and 10 μL was transferred onto two different coupons of freshly cleaved mica (∼1 cm^2). The coupons were dried through absorption of the excess liquid using a lint-free wiper followed by exposure to a moderate vacuum. The dried coupons were transferred to the ARC-PR and exposed to a 100 W, 500 mTorr O_2 plasma or to 500 mTorr O_2 gas (no power) for 3 min each. Samples were then imaged with a Digital Instruments multimode atomic force microscope in tapping mode using a multiwalled carbon nanotube tip (*31*).

Infrared Spectroscopy. A ∼40 mL mid-log phase culture of *D. radiodurans* was harvested (7000 rpm, 5 min), and the cell pellet was completely resuspended in 30 mL of 150 mM NaCl. The washing procedure was repeated twice to remove all constituents of the growth medium, and the final cell pellet was stored at −80 °C. Suspensions of ∼10^{11} cell/mL were prepared by resuspending ca. 10−40 mg of the cells in ca. 20−70 μL of 150 mM NaCl. Microbial films were prepared onto hanging drop slides by adding 6−8 μL of the suspension, followed by drying under moderate vacuum. The dried samples (∼10^9 total cells) were exposed to O_2 or MAG plasmas in the ARC-PR at 100 W and 500 mTorr for 45 min. Control experiments using 500 mTorr of either gas with no applied power were also performed.

After exposure the dried films were resuspended in 20−30 μL of water and transferred to 1.5-mL tubes. The suspension volumes were reduced to ∼5 μL using an Eppendorf Vacufuge, and 10 μL of MeOH was added to each sample. The methanolic suspensions were transferred to KBr optical windows and immediately dried under vacuum to a final pressure of ∼17 mTorr before spectroscopic analysis. The infrared absorption of each sample was measured between 400 and 4000 cm^{-1} using a Nicolet Nexus FT-IR 670 spectrophotometer (2 cm^{-1} resolution, 64 scans). All reactions were completed in triplicate.

Elemental Analysis. *Deinococcus radiodurans* cultures (∼10^9 cell/mL) were prepared as described above and transferred onto tin disks in 10-μL aliquots (∼10^7 cells). Samples were dried and exposed to a 100 W, 500 mTorr O_2 plasma for 0, 1, 10, and 45 min. Carbon analyses on the unexposed and exposed tin disks were performed on a Thermo Quest NA 1100 protein elemental analyzer. The lower limit of detection under these conditions is ∼1 μg of dried cells.

Emission Spectroscopy. A SpectraPro 300i spectrometer (Acton Research) with a SpectruMM CCD Detector (Roper Scientific) was fixed ∼35 cm in front of the reaction chamber of the ARC-PR. The light emitted from the plasma was focused using a quartz lens, and the emission spectrum was recorded between 280 and 930 nm in three steps: (1) 280−400 nm with no filter, (2) 400−700 nm with a 375 nm cutoff filter, and (3) 700−

930 nm with a 650 nm cutoff filter. The glass filters were introduced directly in front of the spectrograph slit to eliminate second-order diffraction of the grating (1200 g/mm). Inverse linear dispersion of the instrument was 2.7 nm/mm, entrance aperture ratio was 0.25 *f*, and slit widths were normally 0.2 mm. Emission spectra for both the O_2 and MAG plasmas at 100 W and 500 mTorr were recorded.

Fresh mid-log phase cultures (2 mL) of *D. radiodurans* were harvested (14,000 rpm, 30 s) and thoroughly resuspended in 1 mL of water. Washing procedure was repeated three times to remove all constituents of the growth medium, and the final cell pellet was resuspended in 30 μL of water. The suspension was transferred to hanging drop slides ($\sim 10^9$ total cells) and dried under moderate vacuum. Samples were exposed to the O_2 plasma at 100 W and 500 mTorr in a closed system. The emission spectra were recorded 3 min after the start of each exposure.

After 40 min, the pressure within the reaction chamber had risen to ~650 mTorr, indicating conversion of the biological matter into the gas phase. A control sample was also prepared using 30 μL of water (no microbes) and exposed to the plasma. Spectra of two duplicate microbial exposures were compared for reproducibility and against the water control to reveal any background contamination.

DNA and Protein Exposure. Plasmid DNA, BSA, and SLO were exposed to O_2 or MAG plasmas at differing powers and the effects assayed using electrophoresis or spectroscopy. Plasmid DNA (pRc/CMV2, 5.5 kb) was dissolved in water to 0.5 μg/μL and added onto hanging drop slides in 2 μL aliquots. The DNA-containing slides were dried under moderate vacuum, transferred to the ARC-PR and exposed to 50−200 W of either plasma for 60 s each. Control experiments were also performed by exposing the dried DNA samples to 500 mTorr of the target gas (no power) and heating the samples to 76 or 55 °C for 60 s each. After exposure, each sample was dissolved in 12 μL of 25 mM HEPES (pH 8.0), and 10 μL was transferred to a 1.5 mL tube containing 2 μL of 6× DNA running dye. All samples were analyzed in parallel by electrophoresis at 80 V using an 0.8% agarose gel in TAE buffer with 0.25 μg/mL ethidium bromide. Gels were visualized by fluorescence (λ_{ex} 302 nm), images were captured, and the DNA bands were quantified using a Epi Chem II Darkroom (UVP, Upland, CA). DNA sizes were estimated by comparison against a 1 kb DNA molecular weight ladder (Invitrogen); the percent change in each DNA band was calculated by comparison with the control. All reactions were completed in duplicate.

BSA was dissolved in water (1 mg/mL), dried onto hanging drop slides in 10 μL aliquots, and exposed to the O_2 plasma (50−250 W, 500 mTorr, 90 s). After exposure, samples were dissolved in 20 μL of 25 mM HEPES (pH 8.0); 10 μL was then removed, mixed with 5 μL of 4× sample application buffer (containing β-mercaptoethanol), and adjusted to 20 μL. All samples were heated at 95 °C for 5 min and separated under denaturing conditions at 150 V using 8−16% polyacrlyamide gradient gel (ISC BioExpress). Gels were stained using Coomassie Brilliant Blue and imaged as described. SLO (1 mg/mL) was added onto hanging drop slides in 5-μL aliquots, dried under moderate vacuum, and exposed to the O_2 plasma (50−200 W, 500 mTorr, 60 s). After exposure, each sample was dissolved in 22 μL of 100 mM sodium borate (pH 9.2); 20 μL was then removed and diluted to 500 μL. Enzymatic activities were measured using ~42 μM linoleic acid in 2 mL of 100 mM sodium borate (pH 9.2). Kinetic reactions were initiated by addition of 100 μL of enzyme, and the change in absorbance at 234 nm was monitored using an Amersham Pharmacia Ultraspec 3300 pro UV−vis spectrophotometer. Enzymatic rates were determined by calculating the initial slopes using Swift II application software. Control experiments were performed by heating samples at 76 °C for 90 or 60 s. All reactions were completed in duplicate.

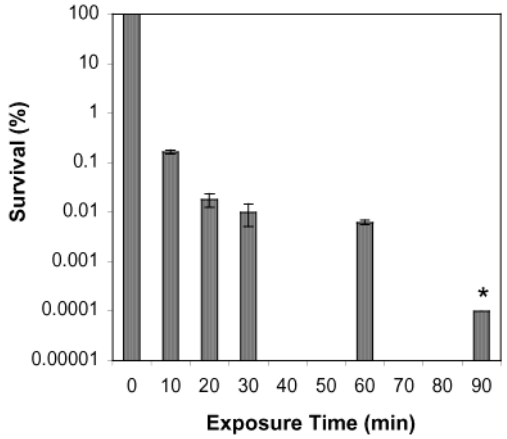

Figure 1. Sterilization kinetics of *D. radiodurans* survival after exposure to O_2 plasma (~25 W, ~45 mTorr). The 90 min exposure (*) yielded no detectable growth; however, the lower limit of detection for most probable numbers method was approximately five cells.

Results and Discussion

Microbe Exposure. *Deinococcus radiodurans* cultures were dried onto polycarbonate membranes and exposed to the O_2 plasma (≤25 W, ~45 mTorr) for 10, 20, 30, 60, and 90 min (Figure 1). Control experiments indicated 68 ± 17% recoveries from the polycarbonate membranes, with negligible effects as a result of drying and the reduced pressures in the plasma reactor (>95% survival). The cell survivability in Figure 1 is expressed in terms of percent survival compared with the control samples.

The 10-min plasma exposure yielded a ~0.1% survival, indicating a ~3-log reduction in living cells, which was further reduced to ~0.001% after 60 min. The 90-min exposure yielded no detectable colony-forming units (0% survival), indicating a complete sterilization of *D. radiodurans*. However, because of the lower limit of detection of five cells (out of an initial $\sim 5 \times 10^6$ cells) when using the most probable numbers method, we have reported the 90 min survival as ~0.0001%. Hence, the final 90-min exposure yielded an overall ~6-log reduction in cell survivability.

The observed difference in sterilization rates between the 10- and 90-min exposures was most likely due to shielding caused by the sterilized cells or the polycarbonate membrane. The shielding effect may be the reason long exposure times are necessary to achieve the ~6-log reduction in bioburden. Using the ARC-PR at 100 W and 500 mTorr, we observed a 0.1% survival after 1 min, indicating that the sterilization rates were effectively expedited at higher power and pressure. Images of *D. radiodurans* were then obtained using atomic force microscopy in order to reveal the degree of structural degradation induced by the O_2 plasma.

Atomic Force Microscopy. Insights into the mechanism of sterilization for *D. radiodurans* were obtained by atomic force microscopy. Images of the control (dried at low pressure) and plasma-exposed cells were compared

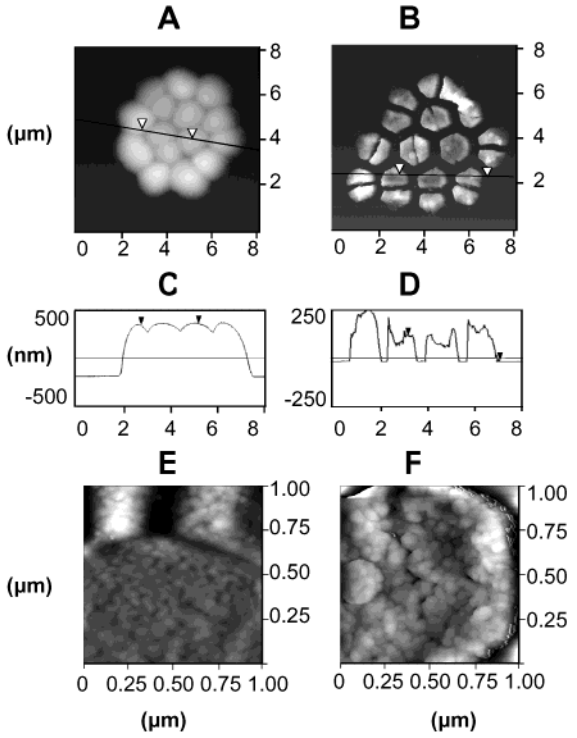

Figure 2. Atomic force microscopy images of a *D. radiodurans* cell cluster (A) dried at 500 mTorr for 3 min and (B) after exposure to O_2 plasma (100 W, 500 mTorr, 3 min). Surface topography maps of (C) the unexposed dried cell cluster and (D) the plasma-exposed cell cluster were obtained across the black line and between the inverted triangles shown in (A) and (B). High-resolution images of (E) one dried cell and (F) a plasma-exposed cell within each cluster were also obtained.

to reveal the changes in cell structure (Figure 2A and B). In the dried unexposed *D. radiodurans* cell cluster the individual cells were ~1.75 μm in diameter, ~0.5 μm in height, and in direct contact with one another. In contrast, the plasma-treated cell cluster (100 W, 500 mTorr, 3 min) showed individual cells to be reduced in size, trapezoidal in shape, and clearly separated from one another. Each plasma-exposed cell was ~1.5 μm long, ~0.5 μm wide, and ≤0.2 μm high.

Topography maps of the unexposed and exposed cells (Figure 2C and D) further indicated the degree of surface degradation. A high-magnification image of a single cell within each cluster (Figure 2E and F) revealed that the surface layer of the unexposed cell was removed or ruptured by the plasma treatment, as indicated by the major change in morphology. The ca. 50- to 70-nm concavities produced by the plasma exposure (Figure 2D and F) are presumably results of the collapse of the degraded surface or of the complete removal of the cell wall and membrane, thereby revealing the dried interior of the cell.

The structural deformation suggested extensive chemical degradation of the microbe through the action of the O_2 plasma. The extents of this molecular damage were then assessed using infrared spectroscopy.

Infrared Spectroscopy. The infrared absorption spectra of *D. radiodurans* (*32*) were measured between 400 and 4000 cm^{-1} (Figure 3). Dried microbial films (~3 mm^2) of *D. radiodurans* (~10^9 cells) were exposed to 100 W of power at 500 mTorr of either O_2 or MAG for 45 min each. A reference spectrum of *D. radiodurans* (Figure 3A) was obtained by performing a control experiment under identical conditions but without the application of power.

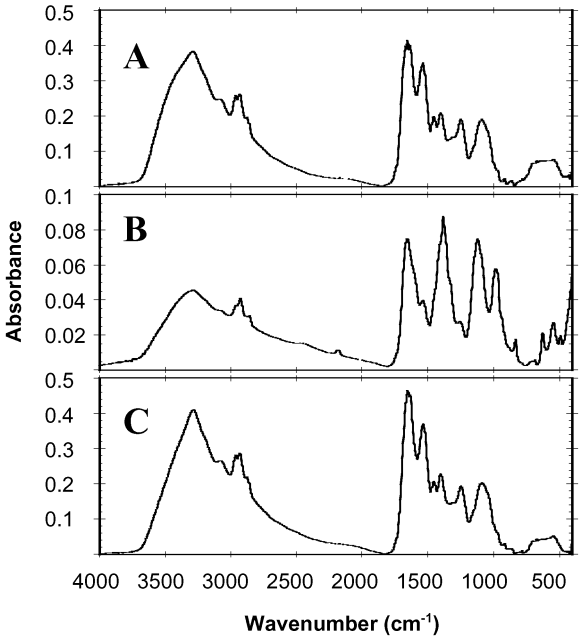

Figure 3. Infrared spectra of *D. radiodurans*: (A) Control sample, (B) sample exposed to O_2 plasma, and (C) sample exposed to MAG plasma. Plasma exposures were performed at 100 W and 500 mTorr for 45 min. Spectra are displayed on differing scales for clarity.

All spectra were normalized to correct for baseline and CO_2 absorption.

Spectral comparison of the plasma-exposed samples against the control revealed three major observations: (1) an ~80% decrease in absorption for the sample exposed to O_2 plasma (Figure 3B), (2) a significant change in the spectral signature between 400 and 2000 cm^{-1} for this sample, and (3) a lack of change for the sample exposed to MAG plasma (Figure 3C).

The ~80% decrease in absorption for the O_2 plasma-treated sample was attributed to the degradation and volatilization of the microbial film as a result of the O_2 plasma chemistry. The decrease in absorption at 2930 cm^{-1} (υ_s CH_2, A ~0.26 to 0.042) was attributed to primary reactions with the lipids and carotenoids of *D. radiodurans*.

Degradation of carotenoids and other biomolecules also correlated with the visible change in sample color and consistency upon exposure, from a red microbial film to a white crustlike material. This chemical change is further supported by the difference in the infrared (IR) spectrum between 400 and 2000 cm^{-1}. The major decrease in absorbance in the amide I/II and conjugated alkene regions (the peaks at 1651 and 1538 cm^{-1}) supported reactions with polypeptides and carotenoids. A major reduction in absorbance was also observed for the asymmetric PO_2^{-1} stretch (1245 cm^{-1}), indicating a loss of DNA or phospholipids. Reduction in absorbance for the C−O stretch and out-of-plane CH bend regions (950−1200 cm^{-1}) also suggested destruction of carbohydrates and carotenoids, respectively.

The observation of new peaks at ~1650, 1384, 1121, and 981 cm^{-1} (Figure 3B) indicated the formation or appearance of additional bonds in the microbial sample. The appearance of peaks at 1384 and 1121 cm^{-1}, however, could also be explained by the presence of residual methanol introduced during sample preparation. The respective peaks do not match those provided in the reference spectra for methanol (1450 and 1033 cm^{-1}) and are of opposite intensities (I υ_s OH 3342 cm^{-1} ≅ I υ_s CO

1033 cm^{-1} > I δ_s CH_3 1450 cm^{-1}) to those observed in the spectra in Figure 3B (I 1384 cm^{-1} > I 1121 cm^{-1} > I 3283 cm^{-1}) (*33*). Neither the spectrum for the control nor the spectrum for the MAG plasma-treated sample contained these peaks, indicating that excess methanol was removed under reduced pressure. We conclude, therefore, that the new IR peaks were resultant of the chemistry between the O_2 plasma and microbial film, as a result of either new bonds forming or low-intensity IR peaks being unmasked.

The change in peak ratios from 1.2 to 1.9 at 1651 and 1538 cm^{-1} can be explained by formation of carbonyl groups on lipids and carotenoids, which would cause an increase in the relative absorbance at ~1650 cm^{-1}. Fragmentation of these molecules could also result in an increase in the CH_3 bend, which is supported by the broad peak at 1384 cm^{-1}. The peaks at 1384 and 1121 cm^{-1} are also suggestive of oxidation of cysteine thiols into sulfonate moieties, whereas the peaks at 1121 and 981 cm^{-1} indicate formation of new C−O bonds within the biological sample.

Overall, these spectral differences indicated the extensive biochemical degradation and removal of *D. radiodurans* as a result of the O_2 plasma exposure. In contrast, the IR spectrum of the sample exposed to the MAG plasma (Figure 3C) showed no detectable degradation or removal of *D. radiodurans*, indicating a significant dependence of degradation on plasma composition.

Elemental analysis on *D. radiodurans* before and after exposure to the O_2 plasma was used to confirm its removal from surfaces. Emission spectroscopy was then used to identify the key reactive species in the O_2 and MAG plasmas and to detect the volatile reaction products resulting from exposure to O_2 plasma.

Elemental Analysis. The extent of removal of *D. radiodurans* from an exposed surface was estimated by elemental analysis. Tin disks were inoculated with ~50 μg of cells and measured for carbon content. A 100 W, 500 mTorr O_2 plasma removed ~40% of the total carbon in 1 min, ~90% in 10 min and ~100% in 45 min. Due to experimental error and instrument sensitivity, these values contain a minimum error of ± 2%.

Emission Spectroscopy. To determine the compositions of the plasmas we placed a spectrometer directly in front of the Pyrex window of the reaction chamber of the ARC-PR and recorded the emission spectra between 280 and 930 nm before and during microbial exposure (Figure 4). The emission spectrum for the pure O_2 plasma discharge (Figure 4A) indicated the presence of excited atomic oxygen, oxygen cation, dioxygen cation, and neutral excited dioxygen at 100 W and 500 mTorr.

Dried films of *D. radiodurans* (~8 mm^2, ~10^9 cells) were then exposed to the O_2 plasma, and the change in the emission spectra was recorded 3 min after the beginning of the exposure (Figure 4B). Comparison of the spectra indicated the formation of several excited species as a result of the degradation of *D. radiodurans*:

- CO_2^+ ($A^2\Pi - X^2\Pi$ system: 287−290, 312−317, 325−330, 337−344, and 351−358 nm)
- CO ($b^3\Sigma - a^3\Pi$ and $B^1\Sigma - A^1\Pi$ systems: 282−284, 296−298, 312−314, 329−331, 347−349, 450−452, 482−484, 518−520, and 559−562 nm)
- N_2 ($C^3\Pi_u - B^3\Pi_g$ system: 316, 337, 357, and 380 nm)
- N_2^+ ($B^2\Sigma_u - X^2\Sigma_g$ system: 392 nm)
- OH ($A^2\Sigma - X^2\Pi$ system: 306−309 nm)
- H (486 and 656 nm)

In addition, sodium (589 nm) and potassium (766 and 770 nm) emission lines were detected, suggesting possible ion bombardment (sputtering) by the O_2 plasma. The shorter wavelengths (UV C, 100−280 nm) such as those emitted by excited phosphorus and sulfur species, were not measured because of absorption by the Pyrex window.

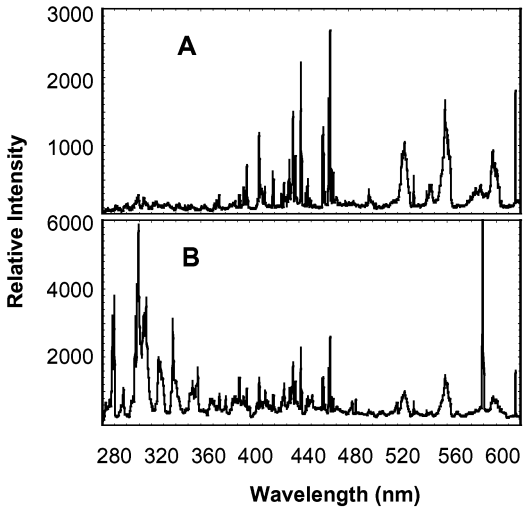

Figure 4. Emission spectra of (A) pure O_2 plasma discharge and (B) plasma during exposure of ~10^9 cells of *D. radiodurans* (100 W, 500 mTorr). Spectra are displayed from 280 to 620 nm and on differing scales for clarity.

The temporal changes in emission spectra indicated that the intensities for CO_2^+, CO, and N_2 increased exponentially with plateaus occurring ~20 min into exposure. Intensities for all O_2 plasma species were stable throughout the experiment, indicating no depletion of reactive oxygen species or parent oxygen gas. Control experiments showed no significant inorganic or organic contamination resulting from sample preparation, glass surface, or water stock, leading us to conclude that all of the detected carbon, nitrogen, and metallic species arose from degradation of the microbial sample.

The emission spectrum for the MAG plasma (data not shown) indicated that several excited species, such as CO_2^+, CO, N_2^+, O, and Ar, were in the plasma. Qualitatively, we observed that the MAG plasma emitted lower intensities of atomic oxygen than the O_2 plasma but significantly higher intensities of UV radiation (UV B) due to emission from CO_2^+ and CO. The effects of these compositional differences on the degradation and removal of biological matter were then assessed using in vitro biochemical experiments.

DNA and Protein Exposure. The extents of biochemical damage imparted by increasing powers of plasma exposure were assayed using model DNA (Figure 5) and protein (Figure 6) systems. In all cases, the samples were solubilized from the exposed glass surfaces using buffer and analyzed by electrophoresis or spectroscopy, which means that insoluble and strongly adsorbed biomolecules were not recovered and therefore not analyzed in this study. Control experiments, however, indicated that DNA was quantitatively recovered from the glass surface. Analysis of catalytic activity indicated approximately 50% recovery of SLO, probably due to adsorption to the glass surface as well as protein denaturation during drying.

Dried ~3-mm^2 films of 1 μg of plasmid DNA were exposed to O_2 or MAG plasmas at 50−200 W and 500 mTorr for 60 s (Figure 5). The increase in power for the O_2 plasma caused a concomitant rise in surface temperatures of the lower electrode in the ARC-PR from ~24 to 72 °C. Therefore, a control sample of DNA was heated to 76 °C for 60 s to indicate the impact of heat on our analyses.

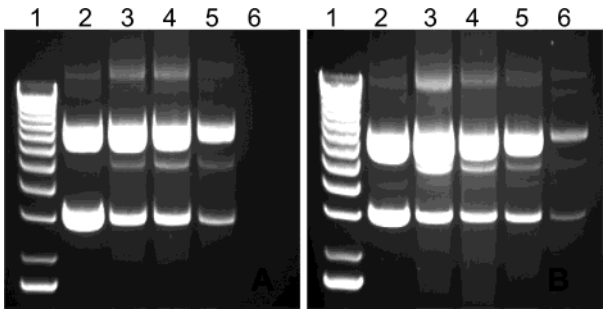

Figure 5. Power-dependent degradation of DNA by (A) O_2 and (B) MAG plasmas (60 s exposures). Lane 1: 1 kb DNA ladder; lane 2: DNA thermal control; lane 3: 50 W; lane 4: 100 W; lane 5: 150 W; lane 6: 200 W.

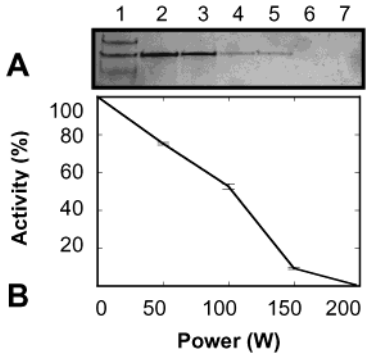

Figure 6. Power-dependent degradation of protein by O_2 plasma: (A) SDS−PAGE analysis of BSA degradation (0−250 W, 500 mTorr, 90 s). Lane 1: molecular weight ladder; lane 2: BSA control; lane 3: 50 W; lane 4: 100 W; lane 5: 150 W; lane 6: 200 W; lane 7: 250 W. (*B*) Kinetic analysis of SLO degradation (0−200 W, 500 mTorr, 60 s).

Lanes 2−6 of Figure 5A show the comparison of thermal versus O_2 plasma degradation of plasmid DNA. Comparison of heated and unheated DNA samples indicated that the experimental temperatures had no measurable effect on the plasmid DNA used (not shown). Upon exposure to 50 W, the amount of supercoiled DNA decreased 32 ± 1% over that of the thermal control, whereas the amount of nicked DNA remained constant within experimental error.

Several new DNA species were produced by the plasma exposure, as indicated by bands at ∼11, 5.5, and 0.5−3 kb. The ∼11 kb band increased ∼14 ± 3% in intensity, suggesting cross-linked DNA formed as a result of the O_2 plasma chemistry. The appearance of a ∼5.5-kb band suggests linear DNA formed as a result of either single- or double-stranded fragmentation of the nicked or supercoiled plasmid, respectively. Multiple double-stranded fragmentation of the DNA was also indicated by the broad ca. 0.5- to 3-kb band.

The higher power exposures of 100 and 150 W caused a ∼5% and 20% decrease in supercoiled DNA, respectively, indicating that ∼50% of the supercoiled DNA remained intact after the 150 W exposure. In contrast, the exposure of 200 W completely degraded all DNA, indicating an approximately 2-fold higher rate of degradation than that observed at 150 W, perhaps due to combined higher production of chemically reactive species, energetic ions, and UV radiation at 200 W.

Exposing dried DNA films to MAG plasma caused degradation patterns similar to those of the O_2 plasma but with differing kinetics (Figure 5B). In these experiments the temperature of the lower electrode ranged from 24 to 54 °C and DNA heat controls were done at 55 °C. Lanes 2−6 of Figure 5B display the effects of heat and MAG plasma on plasmid DNA. In contrast to the O_2 plasma experiments, the exposure to 50 W decreased supercoiled DNA by 48 ± 16% and increased nicked DNA by 8 ± 2%. These findings indicate that single-stranded scission of the supercoiled plasmid occurred, which led to more nicked DNA than in the O_2 plasma experiments.

The 50 W exposure also caused new DNA species to form with sizes corresponding to ∼11, 5.5, and 0.5−3 kb. These bands were again indicative of cross-linked, linear, and multifragmented DNA. The most striking result of the 50 W exposure, however, was the 126 ± 6% increase in cross-linked DNA over the thermal control. Higher power exposures decreased the intensity for all DNA species, yielding a 84 ± 11% reduction in supercoiled DNA at 200 W. Therefore, the MAG plasma did not induce full degradation of the DNA but did result in more detectable fragmentations and cross-linking. Taken together, the difference in degradation rates indicated that the O_2 and MAG plasma compositions contribute differently to the degradation and removal of DNA.

The damaging effects of plasma exposure on polypeptides were also assessed using BSA and SLO (Figure 6). The increasing powers of exposure (50−250 W) caused a nonlinear decrease in the amount of BSA (Figure 6A) and enzymatic rate of SLO (Figure 6B) until each parameter fell below the level of detection. The observed loss of sample and kinetic function were both attributed to oxidation, fragmentation, and removal of the protein as a result of the O_2 plasma chemistry.

Summary and Conclusions

The sterilization efficacy and molecular effects of low-temperature O_2 plasma exposures on *D. radiodurans* and model biomolecules were assessed using microbiological, spectrometric, and biochemical methods. Under very low power and pressure conditions (∼25 W, ∼45 mTorr, 90 min), we have demonstrated a 99.999% reduction in bioburden of *D. radiodurans*, which is resistant to both UV and γ radiation. This ∼6-log reduction of $\sim 10^6$ viable cells reveals the deleterious effects of plasma species such as atomic oxygen.

We also found the rates of *D. radiodurans* killing increased ∼10-fold at higher power and pressure (100 W, 500 mTorr) without the induction of high surface temperatures (∼32 °C). This indicates that plasma power can be adjusted to accommodate the sterilization of both thermolabile (low power, longer exposure times) and robust (high power, shorter exposure times) equipment. Plasma studies on metal (*34*, *35*) and medical (*36*, *37*) materials additionally support the applicability of this technique for spacecraft sterilization.

Killing of *D. radiodurans* occurs as a combined result of damage to the cell surface, the chromosome, and other intracellular components. Atomic force microscopy of *D. radiodurans* shows that exposure to O_2 plasma completely removes or ruptures the cell wall and membrane, revealing the globular interior of the cell. Infrared spectra of the exposed cells indicated chemical degradation of the surface layer, including lipids, carbohydrates, and carotenoids. A major loss in absorbance of the DNA phosphate stretch and amide I/II regions indicates that intracellular damage also occur.

Biochemical experiments show that low-power plasma degrades plasmid DNA via strand scissions and cross-linking to yield nicked, linear, cross-linked, and multifragmented plasmid DNA. Our experiments demonstrate that the rate of DNA degradation is power-dependent and

that a 1-min exposure at 100 W degrades less than 50% of 1 μg of plasmid DNA, whereas at 200 W the DNA is no longer detectable. This finding is significant because *D. radiodurans* can withstand approximately150 strand breaks with no loss in viability (*38*). Hence, a 100-W, 1-min exposure that yielded a ~99.9% reduction of *D. radiodurans* bioburden may not yield the necessary damage to the chromosome of the microbe, indicating that damage to other cellular components must also be a factor in achieving sterilization.

Model in vitro experiments also demonstrate that plasma exposures result in the rapid destruction of protein structure and abatement of enzymatic activity. Taken together, the biochemical experiments reveal a nonlinear increase in degradation rate with increasing power. In addition, they support a sterilization mechanism that proceeds through the degradation of both the surface and interior of *D. radiodurans*.

Our comparison of O_2 and CO_2 plasma experiments reveals that the role of chemical degradation is much greater than that of ion bombardment and UV photodesorption. Our compositional analyses indicate that atomic oxygen is in higher relative abundance in O_2 plasma, as expected, whereas UV-B emissions are higher in MAG plasma.

The considerable difference in degree of microbial degradation ($O_2 \gg$ MAG), as measured by IR, supports the role of atomic oxygen as the dominant source of degradation. The approximate 10-fold increase in DNA cross-linking induced by the CO_2 plasma, however, supports the role of UV as the main source of DNA degradation at plasma powers of $\leq$100 W. The lack of detectable degradation by the CO_2 plasma then indicates that the ion bombardment and UV photodesorption processes are insufficient in imparting significant damage to a robust cell like *D. radiodurans*. The killing and degradation of *D. radiodurans* must proceed through the primary action of reactive species such as atomic oxygen, oxygen cation, and metastable dioxygen species. IR detection of carbonyl, sulfonate, and alcohol reaction products confirms the oxidative degradation of *D. radiodurans* by reactive oxygen species.

Emission spectroscopy experiments showed that *D. radiodurans* degrades into several low molecular weight gases when exposed to O_2 plasma. Conversion of the microbe into CO_2, CO, N_2, OH, and H occurs as a result of the synergistic plasma processes discussed above. Our detection of Na and K emission lines indicate that redox chemistries of free electrons in the plasma also contribute to the observed degradation.

Detection of carbon and nitrogen species in the plasma phase confirms the volatilization of biological matter and supports the observed loss of sample in the IR and biochemical experiments. Removal of *D. radiodurans* was further corroborated by elemental analyses, which indicated a $\geq$98% loss of microbial matter (50 μg) from an exposed surface (100 W, 500 mTorr, 45 min). Complete removal and volatilization of the microbes and biomolecules may be achieved by exposures with O_2 plasma of sufficient duration and power. Detailed analyses of this removal process from surfaces will be the subject for future studies.

In conclusion, our results indicate that O_2 plasmas are effective for removing or reducing bioburden on surfaces. These plasmas have low power requirements and can be adjusted to match material compatibility. Our DNA and protein experiments indicate that O_2 plasmas have application in the sterilization and removal of viruses and protein toxins such as HIV (*39*) and prions (*11*). We have also demonstrated a significant reduction in bioburden of the chemically resistant spores of *Bacillus subtillus* (unpublished data), which supports the general applicability of this technique to differing microbes and biomolecules. From a NASA perspective, O_2 plasma procedures may help meet the need for responsible space exploration and planetary protection. Our experiments with CO_2 plasmas suggest that robust organisms such as *D. radiodurans* may not be significantly degraded in an ionizing Martian atmosphere, which emphasizes the prerequisite need for treating Mars-bound probes.

Acknowledgment

We thank the Mars Advanced Planning Program (NASA) and NASA Faculty Fellowship Program for support, Alessandro Airo and Hiroshi Imanaka for preliminary results, Jeff Ifland for construction of the ARC-PR, Brett Cruden for valuable discussions, and Warren Belisle for the elemental analysis.

References and Notes

(1) Alfa, M. J. Methodology of reprocessing reusable accessories. *Gastrointest. Endosc. Clin. N. Am.* **2000**, *10*, 361−378.

(2) Dempsey, D. J.; Thirucote, R. R. Sterilization of medical devices: a review. *J. Biomater. Appl.* **1989**, *3*, 454−523.

(3) DeVincenzi, D. L.; Stabekis, P.; Barengoltz, J. Refinement of planetary protection policy for Mars missions. *Adv. Space Res.* **1996**, *16*, 311−316.

(4) Rummel, J. D. Planetary Protection Policy (U.S.A.). *Adv. Space Res.* **1992**, *12*, 129−131.

(5) Mann, A.; Kiefer, M.; Leuenberger, H. Thermal sterilization of heat-sensitive products using high-temperature short-time sterilization. *J. Pharm. Sci.* **2001**, *90*, 275−287.

(6) Rutala, W. A.; Weber, D. J. Disinfection of endoscopes: review of new chemical sterilants used for high-level disinfection. *Infect. Control Hosp. Epidemiol.* **1999**, *20*, 69−76.

(7) Jacobs, G. P. A review of the effects of gamma radiation on pharmaceutical materials. *J. Biomater. Appl.* **1995**, *10*, 59−96.

(8) Akterian, S. G.; Fernandez, P. S.; Hendrickx, M. E.; Tobback, P. P.; Periago, P. M.; Martinez, A. Risk analysis of the thermal sterilization process. Analysis of factors affecting the thermal resistance of microorganisms. *Int. J. Food Microbiol.* **1999**, *47*, 51−57.

(9) Hoff, J. C.; Akin, E. W. Microbial resistance to disinfectants: mechanisms and significance. *Environ. Health Perspect.* **1986**, *69*, 7−13.

(10) Buchanan, R. L.; Edelson, S. G.; Boyd, G. Effects of pH and acid resistance on the radiation resistance of enterohemorrhagic *Escherichia coli*. *J. Food. Prot.* **1999**, *62*, 219−228.

(11) Antloga, K.; Meszaros, J.; Malchesky, P. S.; McDonnell, G. E. Prion disease and medical devices. *ASAIO J.* **2000**, *46*, S69−72.

(12) Rutala, W. A.; Weber, D. J. New disinfection and sterilization methods. *Emerging Infect. Dis.* **2001**, *7*, 348−353.

(13) Doue, B. Electron-beam accelerators: a technology adapted for the sterilization of medical devices. *Med. Device Technol.* **1992**, *3*, 48−53.

(14) Dillow, A. K.; Dehghani, F.; Hrkach, J. S.; Foster, N. R.; Langer, R. Bacterial inactivation by using near- and supercritical carbon dioxide. *Proc. Natl. Acad. Sci. U.S.A.* **1999**, *96*, 10344−10348.

(15) Zafar, A. B. A review of the plasma sterilization systems. *Am. J. Infect. Control* **1996**, *24*, 312.

(16) Adler, S.; Scherrer, M.; Daschner, F. D. Costs of low-temperature plasma sterilization compared with other sterilization methods. *J. Hosp. Infect.* **1998**, *40*, 125−134.

(17) Lerouge, S.; Wertheimer, M. R.; Marchand, R.; Tabrizian, M.; Yahia, L. Effect of gas composition on spore mortality and etching during low-pressure plasma sterilization. *J. Biomed. Mater. Res.* **2000**, *51*, 128−135.

(18) Jacobs, P.; Kowatsch, R. Sterrad Sterilization System: a new technology for instrument sterilization. *Endosc. Surg. Allied Technol.* **1993**, *1*, 57−58.
(19) Moisan, M.; Barbeau, J.; Moreau, S.; Pelletier, J.; Tabrizian, M.; Yahia, L. H. Low-temperature sterilization using gas plasmas: a review of the experiments and an analysis of the inactivation mechanisms. *Int. J. Pharm.* **2001**, *226*, 1−21.
(20) Chapman, B. *Glow Discharge Processes*; John Wiley & Sons: New York, 1980.
(21) Demidov, V. V.; Goncharov, A. A.; Osipov, V. B.; Trofimov, V. I. Modern aspects of planetary protection and requirements to sterilization of space hardware. *Adv. Space Res.* **1995**, *15*, 251−255.
(22) Horneck, G.; Facius, R.; Reitz, G.; Rettberg, P.; Baumstark-Khan, C.; Gerzer, R. Critical issues in connection with human planetary missions: protection of and from the environment. *Acta Astronaut* **2001**, *49*, 279−288.
(23) Rummel, J. D. Planetary protection in the time of astrobiology: Protecting against biological contamination. *Proc. Natl. Acad. Sci. U.S.A.* **2001**, *98*, 2128−2131.
(24) Lange, C. C.; Wackett, L. P.; Minton, K. W.; Daly, M. J. Engineering a recombinant *Deinococcus radiodurans* for organopollutant degradation in radioactive mixed waste environments. *Nat. Biotechnol.* **1998**, *16*, 929−933.
(25) Venkateswaran, A.; McFarlan, S. C.; Ghosal, D.; Minton, K. W.; Vasilenko, A.; Makarova, K.; Wackett, L. P.; Daly, M. J. Physiologic determinants of radiation resistance in *Deinococcus radiodurans*. *Appl. Environ. Microbiol.* **2000**, *66*, 2620−2626.
(26) Davies, K. J. Protein damage and degradation by oxygen radicals. I. general aspects. *J. Biol. Chem.* **1987**, *262*, 9895−9901.
(27) Peskin, A. V. Interaction of reactive oxygen species with DNA. A review. *Biochemistry (Moscow)* **1997**, *62*, 1341−1347.
(28) Garrison, W. M. Reaction mechanisms in the radiolysis of peptides, polypeptides and proteins. *Chem. Rev.* **1987**, *87*, 381−398.
(29) Caimi, P.; Eisenstark, A. Sensitivity of *Deinococcus radiodurans* to near-ultraviolet radiation. *Mutat. Res.* **1986**, *162*, 145−151.
(30) Hieda, K.; Suzuki, K.; Hirono, T.; Suzuki, M.; Furusawa, Y. Single- and double-strand breaks in pBR322 DNA by vacuum-UV from 8.3 to 20.7 eV. *J. Radiat. Res. (Tokyo)* **1994**, *35*, 104−111.
(31) Stevens, R.; Nguyen, C.; Cassell, A.; Delzeit, L.; Meyyappan, M.; Han, J. Improved fabrication approach for carbon nanotube probe devices. *Appl. Phys. Lett.* **2000**, *77*, 3453−3455.
(32) Melin, A. M.; Perromat, A.; Deleris, G. Sensitivity of *Deinococcus radiodurans* to gamma-irradiation: a novel approach by Fourier transform infrared spectroscopy. *Arch. Biochem. Biophys.* **2001**, *394*, 265−274.
(33) Silverstein, R. M.; Bassler, G. C.; Morrill, T. C. *Spectrometric Identification of Organic Compounds*; 5th ed.; John Wiley & Sons: New York, 1991; p 151.
(34) Belkind, A.; Li, H.; Orban, Z.; Jansen, F. An in situ XPS study of oxygen plasma cleaning of aluminum surfaces. *Surface Coatings Technol.* **1997**, *92*, 171−177.
(35) Aronsson, B. O.; Lausmaa, J.; Kasemo, B. Glow discharge plasma treatment for surface cleaning and modification of metallic biomaterials. *J. Biomed. Mater. Res.* **1997**, *35*, 49−73.
(36) Goldman, M.; Pruitt, L. Comparison of the effects of gamma radiation and low-temperature hydrogen peroxide gas plasma sterilization on the molecular structure, fatigue resistance, and wear behavior of UHMWPE. *J. Biomed. Mater. Res.* **1998**, *40*, 378−384.
(37) Kelly-Wintenberg, K.; Montie, T. C.; Brickman, C.; Roth, J. R.; Carr, A. K.; Sorge, K.; Wadsworth, L. C.; Tsai, P. P. Y. Room-temperature sterilization of surfaces and fabrics with a one atmosphere uniform discharge plasma. *J. Ind. Microbiol. Biotechnol.* **1998**, *20*, 69−74.
(38) Daly, M. J.; Ouyang, L.; Fuchs, P.; Minton, K. W. In vivo damage and recA-dependent repair of plasmid and chromosomal DNA in the radiation-resistant bacterium *Deinococcus radiodurans*. *J. Bacteriol.* **1994**, *176*, 3508−3517.
(39) Smith, R. A.; Ingels, J.; Lochemes, J. J.; Dutkowsky, J. P.; Pifer, L. L. Gamma irradiation of HIV-1. *J. Orthop. Res.* **2001**, *19*, 815−819.

Accepted for publication February 5, 2003.

BP025665E